REVIEW

Check for updates

State-of-art plasmonic photonic crystals based on self-assembled nanostructures

Ashish Yadav, [iD] *[a] Neha Yadav,[a] Vikash Agrawal,[b] Sergey P. Polyutov, [iD] [c] Alexey S. Tsipotan, [iD] [c] Sergei V. Karpov, [iD] [cd] Vitaliy V. Slabko,[c] Vikram Singh Yadav,[e] Yongling Wu,*[a] Hongyu Zheng*[a] and Seeram RamaKrishna [iD] *[f]

Controlled self-assembly of plasmonic photonic nanostructures provides a cost-effective and efficient methodology to expand plasmonic photonic nano-platforms with unique, tunable, and coupled optical characteristics. Keeping advantages and challenges in view, this review highlights contemporary advancements towards the development of self-assembly of a plasmonic photonic nanostructure using a colloidal solution and a self-assembly modeling technique along with exploring novel optical properties and associated prospects. The potential applications of self-assembled plasmonic photonic nano-systems to investigate next-generation optoelectronic devices, the need to reduce and increase scaling up aspects, and improve the performance, are also covered briefly in the review. The need of considerable efforts for the design and development towards establishing novel cost-effective methods to fabricate controlled self-assembled smart nano-plasmonic platforms is also highlighted in this mini-review. Key confronting issues that precisely limit the self-assemblies of photonic nanostructures and desired integration with other device components, mainly including uniformity within miniaturized devices are also discussed. This review will serve as a guideline and platform to plan advanced research in developing self-assembled plasmonic photonic nano-systems to investigate smart functional optical devices.

1. Introduction

Photonics has attracted sufficient attention in the scientific community as a critical cross-disciplinary arena of science and technology with an emphasis on the controlled propagation and tactical manipulation of light.[1–4] The credit of the recent advancement in photonics can be attributed to the improved understanding of optics, nanotechnologies, plasmonics, physics, and materials science but not limited to the constant and rapid developments of microfabrication techniques.[5–7] It is the outcome of the interaction of periodic modulation in the structure of plasmonic materials with light, which produces a wide range of

[a] *Center for Advanced Laser Manufacturing (CALM), Shandong University of Technology, Zibo, 255000, P. R. China. E-mail: ashish84yadav@gmail.com, zhenghongyu@sdut.edu.cn*

[b] *School of Physics, Southeast University, Jiangning District, Nanjing 211189, People's Republic of China*

[c] *Siberian Federal University, 660041, Krasnoyarsk, Russia*

[d] *Kirensky Institute of Physics, Federal Research Center KSC SB RAS, 660036, Krasnoyarsk, Russia*

[e] *Department of Applied Sciences, Bundelkhand Institute of Engineering and Technology, Jhansi, India*

[f] *Nanoscience and Nanotechnology Initiative, National University of Singapore, 10 Kent Ridge, Crescent 119260, Singapore. E-mail: seeram@nus.edu.sg*

new and sometimes completely unique results.[8] These outstanding results lead the pathway towards promising applications in the construction of optical resonators, Bragg mirrors, filters, and switches.[9–11]

Plasmonics-based photonic crystal (PC) devices[12] play an essential role in the upcoming technology, leading to smart devices, and it may fill the gap between conventional photonics and microelectronics.[13–15] The substantial miniaturization of nano-scale components for existing computational and information storing devices has only been possible due to the tunable electrical properties of semiconductor materials. However, the resistance–capacitance (RC) delay-time issues of interconnects severely limit the speed in semiconductor electronics, and the fundamental diffraction laws of light put a limit in the use of photonics.[16–18] Plasmonics might come out to be a solution to both problems, *i.e.*, further reduction of the size of electronics and enhancement in the speediness of photonics. Plasmonic devices probably work as a bridge between the speed limit of photonic chips and the size limit of semiconductor electronic components, thereby providing a perfect balance between two surviving technologies.

Plasmon-based photonic crystals contribute significantly to the development of materials for plasmonic photonic nanostructures.[19–21] This variety of materials are comparatively

3368 | *J. Mater. Chem. C*, 2021, **9**, 3368–3383

This journal is © The Royal Society of Chemistry 2021

low-priced, which can be chemically modified to exhibit desirable characteristics either optically, electronically, or mechanically, and the best part is that they have already proved their suitability with a library of designed nanostructures.[22–26] These nanostructures may serve as building block materials in numerous ways for photonic applications. First, plasmonic PCs may exhibit suitable nonlinear optical properties and the desired range of electroluminescence or photoluminescence,[27–30] Second, plasmonics-based PCs can serve as frameworks for optically active materials, including, dyes and liquid crystals.[31–34] Recent works, research outcomes, glitches, and opportunities to develop the plasmon-based photonic nanostructured substances towards applications in photonics and optically assisted data storage devices[35,36] were emphasized in this review. However, this review is restricted to materials whose nanostructured photonic properties originated from a periodic variation in composition or configuration.

Based on these, nanophotonic structures and gadgets are expected to bring increasing improvements in the case of low-energy consuming devices in subsequent decades,[37] a betterment in the spatial-resolution for much better images, designing of novel highly sensitive sensors for specific requirements, and producing integrated information systems with a capacity to hold mass-scale data at a much lesser power consumption.[38] Advancements and an improved understanding regarding the design of miniaturized optical structures at nano-scale level, enhanced skills towards tailoring the desired properties of materials, and better grasp of the nature of light–matter interactions lead scientists in understanding the probable viability of nanophotonics towards the realization of sophisticated gadgets, and this strongly inspires further research possibilities in this field.[3] Well-known lithography techniques were dominated to fabricate photonic nanostructures before the last decade. However, the recent improvements and better understanding of self-assembly approaches have paved several new pathways for the large-scale miniaturization and minutely controlled fabrication of the vast arrays of homo-generous and nano-patterned surfaces as well as resource materials.[39–42]

2. Self-assembly based on the plasmonic nanostructure

The plasmonic nanostructures could be attached in the form of self-assemblies in various manners, with a difference in nano-particle (NP) structures, their individual shapes, and sizes (as illustrated in Fig. 1). This method may also be useful for mass-scale production. The primary driving nanoscale forces, responsible for the precise control of nanostructures, e.g. capillary forces, centrifugal force, repulsive interactions, and spin-speed, primarily affect the self-assembly route and the final nanostructured ensembles.[43–45]

Plasmonic photonic nanostructured materials can be produced in high quality by self-assembly. There are mainly two approaches, top-down and bottom-up for the fabrication of plasmonic photonic nanostructured materials, briefly discussed as follows:

(A) The top-down approach, in which the final structure of photonic crystals (PCs) in highly precise resolution can be achieved using the lithography techniques employing electrons, ions, atoms, and photons, in addition to embossing and scanning tip methods. However, this approach is quite costly, and the sequential nature of the top-down approach demands comparatively more extended time to achieve the final structure over larger surfaces.[47–49]

(B) The bottom-up approach, in which the ordered periodic structures count on the self-driven assembly of elementary construction labs. The approach is generally much more efficient in terms of speed, cost, and mass-scale production than the top-down approaches. However, the top-down methodology is much capable in terms of precise regulation and desired accuracy during the fabrication of the very final structure.[50,51] The lesser price and easy fabrication make bottom-up approaches to be viable and real-world choices that could compete with top-down approaches. Fabrication methods to produce such excellent quality final structures using conventionally available methods have been a colossal task in earlier times; however, the latest understanding of the subject, new fabrication techniques, and modern available research tools have solved the problems to a much larger extent. However, it is still a struggle to find out an approach to precisely fabricate the structures at a mass scale and even much lower costs and have a much more accurate control towards the targeted structures. Probably, the colloidal self-assembly is the most frequently embraced fabrication methodology to design and chemically fabricate PC structures. Some latest and most sophisticated features regarding the colloidal self-assembly of PCs are addressed in the following sections (Table 1).

2.1 Colloidal self-assembly

Polymeric anisotropic mono-disperse particles are fabricated by the bottom-up methodology. Tiny building blocks work with colloidal forces in the colloidal assembly. Sedimentation is one of the methods to fabricate the direct assembly of PCs onto the substrates. It is the most commonly used and the most basic simple approach. Natural opals are also formed by sedimentation under gravity on the tiny particles that build the opal.[52] Alternatively, in the drop-cast method, drops of colloidal suspension are released onto the surface of the substrate and dried until evaporation.[53] The repulsive forces between the charges hinder the premature aggregation of particles. As an example, electrostatic repulsion in polar solvents promotes the stabilization of charges.[54,55] A wise choice of substrate, proper concentration of suspension, precise control on temperature and humidity may lead to the fabrication of high-quality colloidal crystals. Fig. 2 shows Au@PS NP core–shell-type nanostructures, which are useful for optical devices.

Colloidal crystals were fabricated by two methods: centrifugation and spin-coating. The centrifugal forces are used to bring the particles more closed in a colloidal suspension. The colloidal suspension is allowed to spin at a fast rotation speed in a centrifuge to bring the particles closer or to make them denser. This approach results in excellent quality bulk colloidal

This journal is © The Royal Society of Chemistry 2021

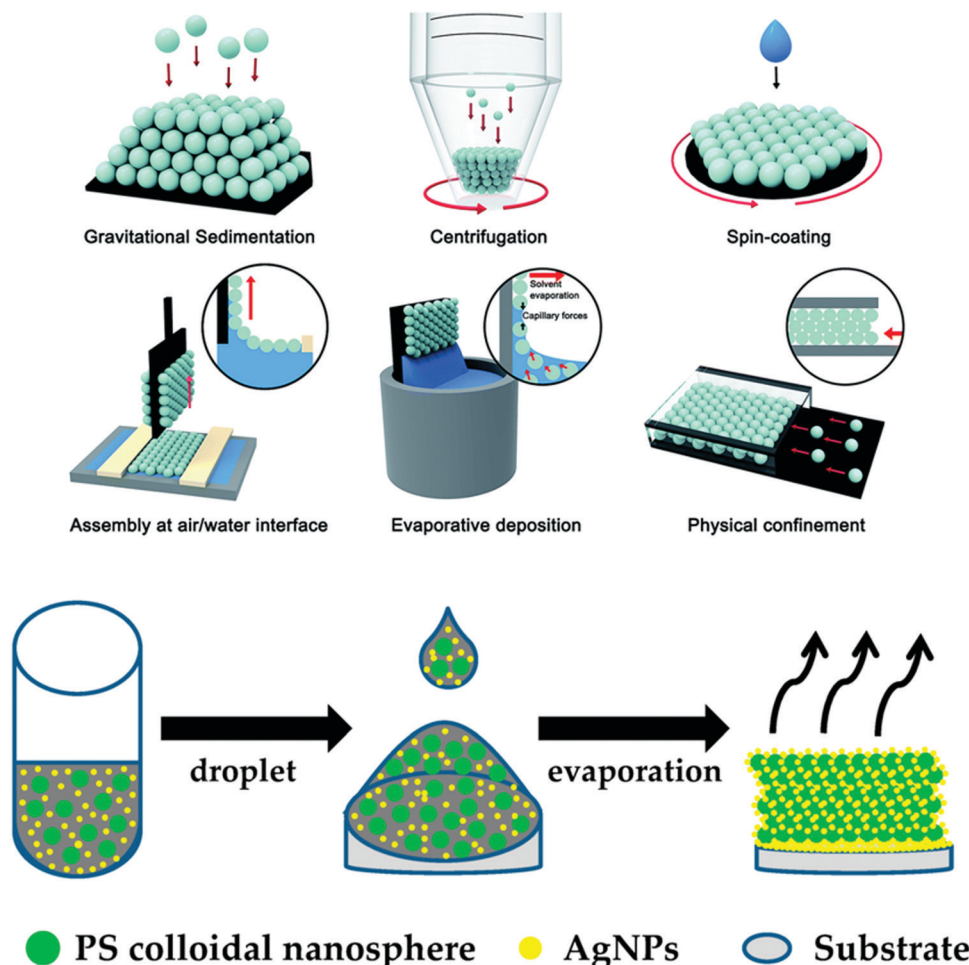J. Mater. Chem. C, 2021, **9**, 3368–3383 | **3369**

Fig. 1 Schematic of the self-assembly of nanostructures; polystyrene colloidal spheres and gold nanoparticles attached with colloidal crystals. Reproduced with permission, Copyright 2016 IntechOpen Press.[46]
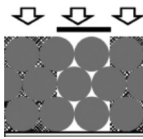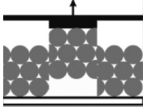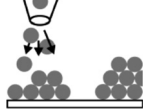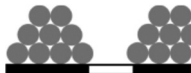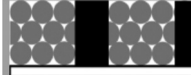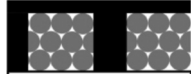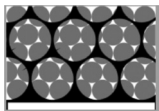
crystals.[55] Contrastingly, on planar substrates, these films or monolayers of colloidal crystals are deposited by spin coating.[56–60] However, the spin-coated films vary on the substrate, with their position from the rotation axis, as different parts of the substrate sense a different force of suspension. The films of colloidal crystals are generally irregular and patchy appearance over the substrate. Jiang *et al.* established a versatile, cost-effective, and modest spin-coating procedure that is modular and well-suited with typical top-down microfabrication. Additionally, Jiang *et al.* also testified the option to manufacture non-closely packed colloidal crystal arrays in two-dimensions (2D) from the spin coating.

2.1.1 Structural color originated from self-assembled colloids. Structural color may be termed as an optical consequence when submicroscopic structure reflects or scatters the selected wavelengths of light. Colloidal-based assembly structural color materials are inspired by nature and are creating a broad research interest over a wide range,[54–57] which can be seen in Fig. 3. The assembly of colloidal particles based on three-dimensional structural color materials provides a cost-effective and straightforward strategy. Various general mechanisms regarding the structural colors from the colloidal assembled

photonic crystalline structure (PCS) have been suggested in the literature. Surface topography, the spatial extent, and narrow-order structures may be used to tailor the optical characteristics of PCSs. An explanation of the controlled variation of structural color can be given by refractive index and lattice distance. Out of several current applications of colloidally assembled structural color materials, a few may be termed bio-substances, microfluidic chips, sensors, flexible and curved displays, and anti-counterfeiting materials.[58–61]

The vertical deposition is a very efficient method to prepare single or several monolayer(s) of ordered colloidal crystals, in which films are deposited onto a vertical substrate by fine-tuning the parameters such as concentration of the colloidal solution, its temperature and humidity. Here, it is worth mentioning the importance of the rate of solvent evaporation, as changing the concentration of the solution results in the change of thickness of colloidal crystals towards the direction of growth. This effect is due to the fact that the colloidal crystals, once deposited on the substrate, automatically induce low occupancy toward the total number of particles in the solution. Another effective methodology for the preparation of monodisperse colloidal particles is field-induced self-assembly.

Table 1 Comparison study of top-down and bottom-up methods

| Method	Schematic	Remarks
Top-down method		
Photo lithography		Photo polymerization of monomer in colloidal crystal assembly 2D and 3D patterning possible, different particles and periodicities combination.
Microimprint lithography		Interplay of adhesion between particles and particles/substrate important, different particles and periodicities combination.
Printing/plotting		Printing of confined structure and controlled drying rounded edges due to drying.
Bottom-up method		
Surface functionalization		Wetting contrast between hydrophilic and hydrophobic areas.
Large topographic pattern		Capillary forces-aided infiltration of trenches.
Microfluidic channels/micro-molding		Infiltration and drying in closed channel.
3D molding		Additional structuring in all three space dimensions.
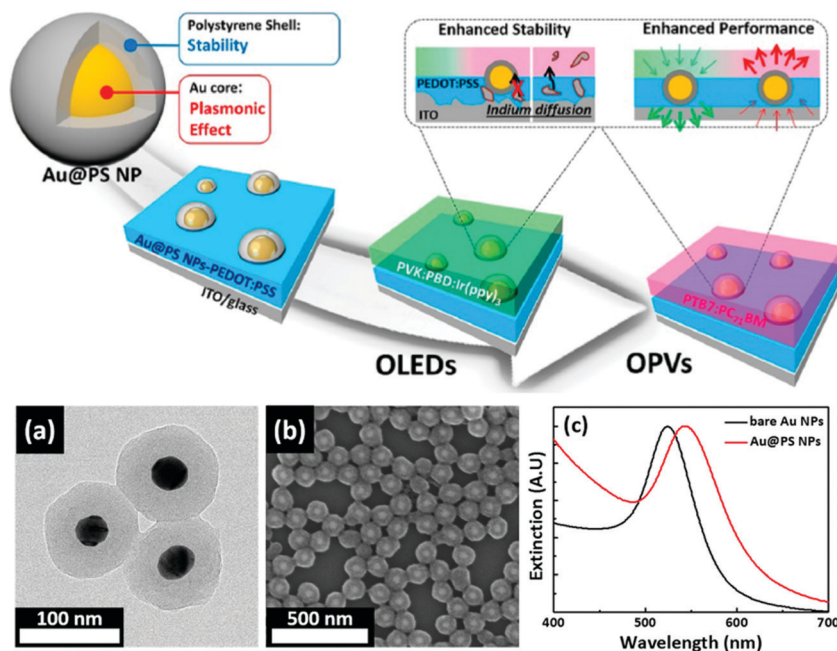
Fig. 2 Schematic of experimental approaches towards Au@PS NPs for OLEDs and OPVs. The Au@PS NPs were incorporated into the PEDOT:PSS film. (a) TEM and (b) SEM images of Au@PS NPs and (c) UV-vis absorption spectra of Au NPs and Au@PS NPs.[53] Reproduced with permission, copyright American Chemical Society.[53]
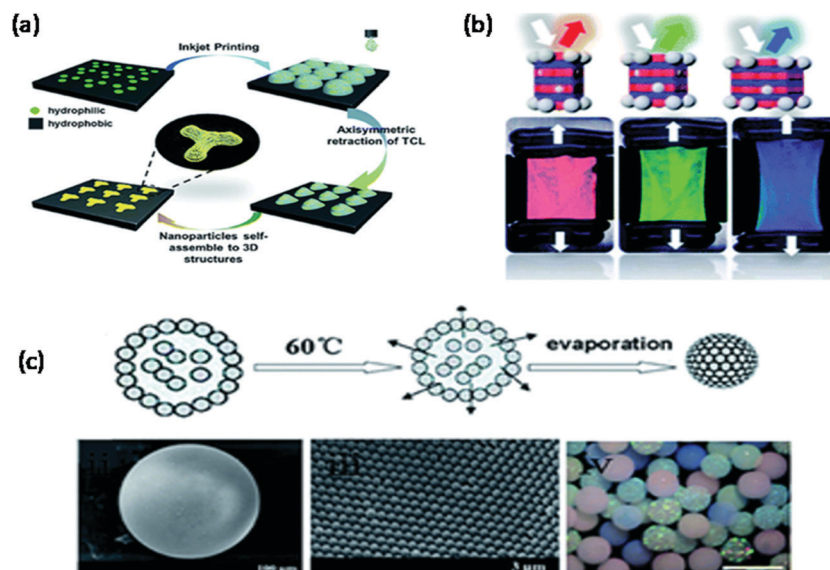
Fig. 3 Three-dimensional PCSs hydrophilic–hydrophobic patterned substrate. (a) Processing the assembly of particles into a microsphere. (b) Representation of the different structural colored microspheres. (c) A non-closely packed fcc arrangement of silica particles in a photonic film and SEM images. Reproduced with permission from the Royal Society of Chemistry.[62]

Woodcock *et al.*[63] successfully used gravity deposition to prepare the PCSs and also presented a detailed theoretical framework regarding the colloidal assembly.[62]

The skillful alteration of surface properties of the substrate surface makes possible the selective and controlled sedimentation of colloidal particles over the surface of the substrate.[64,65] Braun and coworkers used lithography to etch Si substrates and then directly deposited[66] colloidal particles onto it and successfully prepared patterned crystalline colloidal arrays. Ozin and coworkers[67] successfully created surface-confined patterned templates by using a patterned PDMS elastomeric stamp. There are several methods available to pattern the substrates, and high-resolution structures of colloidal PCS can be induced to fabricate over the patterned substrates. The so-obtained substrates may display lively structural colors.

Moreover, a droplet comprising numerous monodisperse colloidal particles, over a 2D patterned substrate, could be employed to form a 3D template for the deposition of spherical PCSs, followed by the evaporation of the solvent. Yang *et al.*[68,69] used microfluidic technologies to combine with the droplet template process to deposit monodisperse microspheres of colloidal crystals. High temperatures enhanced the bonding between the colloidal particles, yielding a more stable microsphere. Smooth standard hexagonal structure microspheres of the colloidal particles can be prepared using this process.[70–72]

2.1.2 Plasmon-based self-assembled nanostructures. A category of periodically varying index of photonic materials called PC may modulate the localized electric fields effectively and has been effectively applied to improve[73–75] the luminescent intensity. Combining photonic crystal effects with surface plasmon (SP) may dramatically improve the luminescent intensity of upconversion nano-phosphors (UCNPs), and it has already resulted in an innovative device. The upconversion luminescence (UCL) of $NaYF_4$:Yb^{3+},Er^{3+} NPs was substantially modulated by gold nanorods (AuNPs)/polymethylmethacrylate (PMMA) opal photonic crystals (OPCs) and surface plasmon photonic crystal (SPPC) (Fig. 4), resulting in as a flawless combination of PC properties of 3D PMMA opals and surface plasmonic effect of AuNPs.[76]

The composition, size, and shape of a metal NPs, combined with the refractive index of the dielectric medium around this metal NP determine both the frequency and the intensity of localized surface plasmon resonance (LSPR), while the inter-particle distance is smaller or nearly of the same order, as of the light wavelength used, different plasmon modes can interact with each other by the near-field coupling within the metal NP assemblies, due to the transfer and confinement of electro-magnetic energy.[76–78]

The similar findings of theory and experiments evaluated the relationship between the dynamic structural properties of AuNR assemblies and their ensemble-averaged surface-enhanced Raman scattering (SERS) characteristics. The finite-element method (FEM) and finite-difference time-domain (FDTD) method were applied together to estimate the optical properties and the electric field improvement of several self-assembled plasmonic assemblies. The results of numerical calculations were in accordance with analytical methods and could be used successfully to evaluate the optical characteristics and electric field profiles of remarkable plasmonic assemblies,[79–82] which were not yet verified within the laboratory. Lots of commercial software are available for the electromagnetic simulation, *e.g.* XFDTD, HFSS, Lumerical FDTD simulations, FEM-based software, and ComsolMultiphysics (RF module). Meep (an acronym for MIT electromagnetic equation propagation) is an example of an open-source software package. Accurate simulations for self-assembled plasmonic structures ought to rely on suitable numerical techniques. The approach's option is contingent on the problem of the resources, in addition to interest.
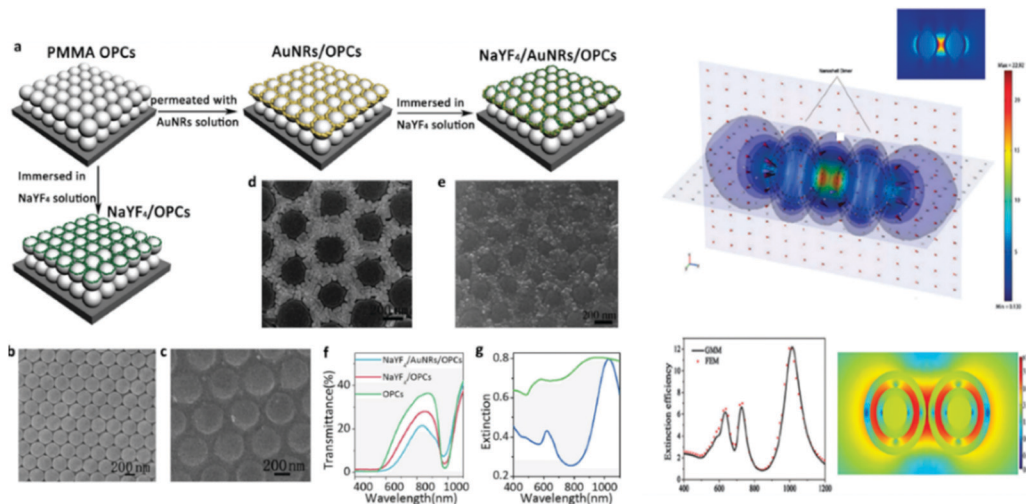
3372 | *J. Mater. Chem. C*, 2021, **9**, 3368–3383

This journal is © The Royal Society of Chemistry 2021

Fig. 4 (a) Graphic diagram of the SPPC assembly, NaYF$_4$/AuNR/OPC hybrid structure, and NaYF$_4$/OPC hybrid fabrication method. SEM diagrams of (b) PMMA opal OPC and (c) NaYF$_4$/OPCs hybrid structures. The 3D schematic of electric field effect near a gold nanoshell dimer by FEM is given. (d and e) Inverse structure of NaYF$_4$/. The 2D slice plot for reference purposes is shown in the inset. (f) Comparing the calculated extinction and near-field experimental findings of GMM theory and FEM for a dimer of multilayer metal–dielectric nanoshells. (g) PL of hybrid nanostructures NaYF$_4$. Reproduced with permission from Wiley Publications.[76]

The successful implantation of AuNRs into the periodic surface gaps of 3D PMMA OPCs shows a dramatic amplification in the local electric field because of the combined influence of SPR and PC. This distinguishing SPPC structure was analyzed to improve the UCL of NaYF4:Yb^{3+},Er^{3+} UCNPs by the added accumulation of the UCNPs over the exterior of AuNRs/OPCs composites.

3. Modeling the self-assembly nanostructure process

The metal particles ranging in the nanometer size have gained significant interest in the late decade due to their exceptional optical properties. Plasmonic metal NPs have shown significant gains in numerous applications, *e.g.* nanofabrication industries,[83] optical communication,[84] and biological detection.[85,86] Due to the outstanding electromagnetic field augmentation from LSPR, and SERS on metal nanoparticles, they are deemed to be an effective analytical instrument in chemical and biological investigations for understanding the molecular information, *e.g.* chemical composition, chemical bonding, and orientation of crystals.[87]

Wafer-scale and uniform plasmonic substrates can be fabricated at a very minimal price tag for the best performance in SERS applications. This recently developed method is tunable,[88] uses a metal thin-film thermal dewetting procedure and does not require lithography for nanofabrication. The association between tunable process parameters and the similar plasmonic and optical characteristics is verified using both experiments and theory to understand and determine the design of an optimal SERS device comprising a 3D plasmonic nano-antenna structures.[88]

Thermal dewetting is a simple bottom-up self-assembly technique for producing SC metal NPs from PC-metal thin films, which includes the most common metals for nano-plasmonics. This procedure provides a simple self-assembly technique to fabricate a plasmonic device for SERS applications as well as, it adds the flexibility features in these devices. The relationships between plasmonic phenomena and equivalent tunable geometric parameters have been theoretically understood on the basis of FDTD simulations and optical characteristics. The shape, size, and emergence of the supported nanostructure could substantially affect the properties of plasmonic structures. The thermally dewetted AuNPs having thicker Au layers become more substantial in size and produce red-shifted LSPR modes. The increased dewetting temperature delivers more thermal energy to create spherical AuNPs with a better LSPR holding capacity. A nanostructured substrate encourages the trapping of light as well as the electric field near the surface, as shown in Fig. 5.

4. Plasmon-based hybrid metal–semiconductor nanostructures

The flow of electromagnetic energy on the nanoscale extents may be controlled skillfully by combining the optical properties of semiconductor and metal nanostructures. When the semiconductor nanostructures and dielectric-restricted electromagnetic modes in the metal analogues are brought closer at the nanoscale neighborhood, in the form of heterostructures, both material systems contribute to interactions between respective quantum-confined electronic states.

Plasmon interactions can help to successfully re-design the absorption and emission characteristics, increment of optical nonlinearities within the medium, production of novel
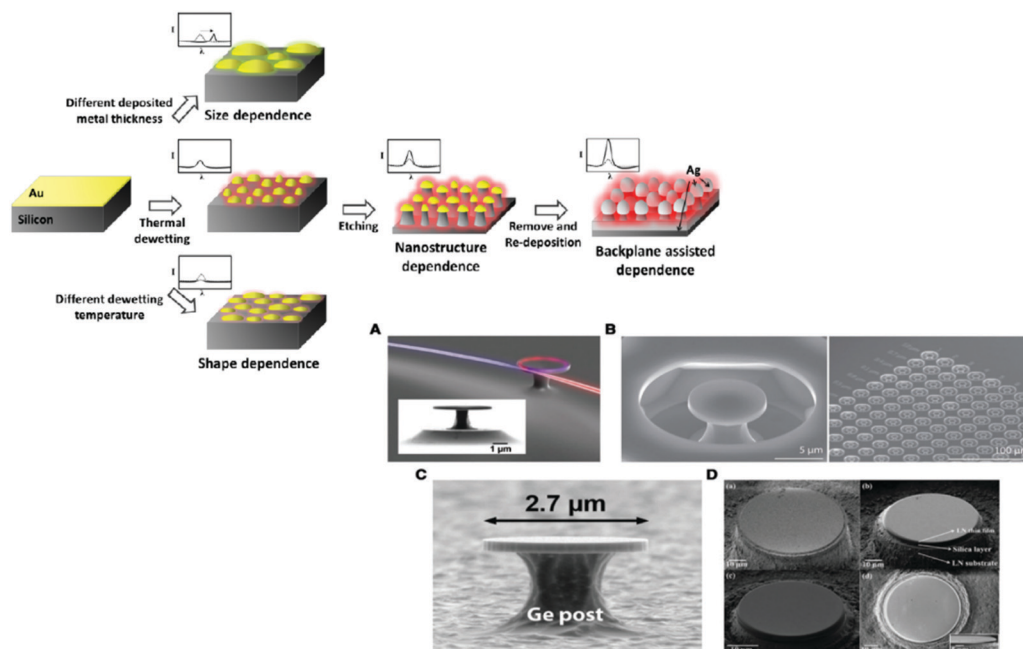
This journal is © The Royal Society of Chemistry 2021

J. Mater. Chem. C, 2021, **9**, 3368–3383 | **3373**

Fig. 5 Outline of the dependence of plasmonic augmentation by controlling several process parameters during the fabrication including the morphology of metal NPs, the emergence of nanostructures, and the backplane-aided effects. Optical microdisk resonators (A) SEM micrograph of a GaAs micro-disk and representation of the fiber-taper-coupling-based second-harmonic generation. Reprinted from ref. 89. (B) SEM micrograph of a single monolithic diamond microdisk and an arrangement of these structures. Reprinted from ref. 90. (C) SEM micrograph of a pseudomorphic quantum-well micro-disk with a Ge post. Reprinted from ref. 91 and 92. (D) SEM micrographs for lithium-niobate micro-resonators. Reproduced with permission from SPIE Digital Library.[18]

excitations in the robust coupling regime, and careful regulation of energy-transfer phenomena at nanoscale levels. The development of sophisticated fabrication techniques at microscale levels could help tremendously to govern the performance of metal–semiconductor nano-assemblies and to control the optical properties and energy flow on length-scales in nanometers and time-scales in femtoseconds.

The combination of metal NPs with semiconductor counterparts originates new path ways to fabricate and design novel, versatile, and highly efficient nanomaterials by unifying individual magnetic and electronic properties of plasmonic NPs.[93] NP interaction with building blocks may give rise to some novel characteristics in materials, in addition to the straightforward combination of NP properties. The amalgamation of plasmonic NPs with hybrid clusters containing semiconductor quantum dots (QDs) may couple the excitonic properties of QDs with the plasmonic properties of metal NPs and the resulting nanostructure may have all new optoelectronic properties.[94,95]

The nanostructures containing QDs are attractive for the creation of nonlinear optical materials (*e.g.* laser shutters and radiation converters), as well as new generation of materials for electronics and photonics and corresponding devices such as light-emitting diodes, solar cells and field effect transistors. The majority of papers devoted to self-organized formation of nanostructures are based on the chemical interactions featured by the selectivity with respect to the molecular content of the particles from which they are formed.[96] Another approach is the self-organization based on physical effects, for example, electrodynamic interaction between NPs for the sake of external

AC electric field – optical binding,[97] or the interaction of the particles with gradient field – optical trapping.[98] These methods, however, possess a number of disadvantages connected with the inability to form the structures of NPs made of different materials, as well as with their subsequent replication.

In ref. 93, authors suggested an approach based on the self-organization of NPs made of metals, semiconductors and dielectrics, under the action of quasiresonant laser irradiation. Note that isolated nanoparticle's resonant frequency depends on their chemical compounds and size.

Interaction of particles in the laser field leads to the shift of their resonant frequencies, and this shift depends on the distance between particles and mutual orientation of the particles with respect to the laser field polarization. The proper selection of a laser radiation frequency allows increasing colloidal nanoparticles attraction to a value which exceeds both the thermal motion and stabilizing potential barrier. This approach allows obtaining structures of different contents with a given geometry of the arrangement, being free of disadvantages noted above, and having no analogs. A series of theoretical, computational and experimental studies connected with investigation of photophysical and nonlinear-optical properties of fractal nanostructures composed of metal (silver) nanoparticles with a resonance in the visible were conducted earlier. Subsequently, conceptions developed as a result of these studies led to the suggestion of the possibility of self-organization of nanostructures with a pre-defined configuration controlled by resonant laser irradiation;[99] recently, preliminary experiments

3374 | *J. Mater. Chem. C*, 2021, **9**, 3368–3383

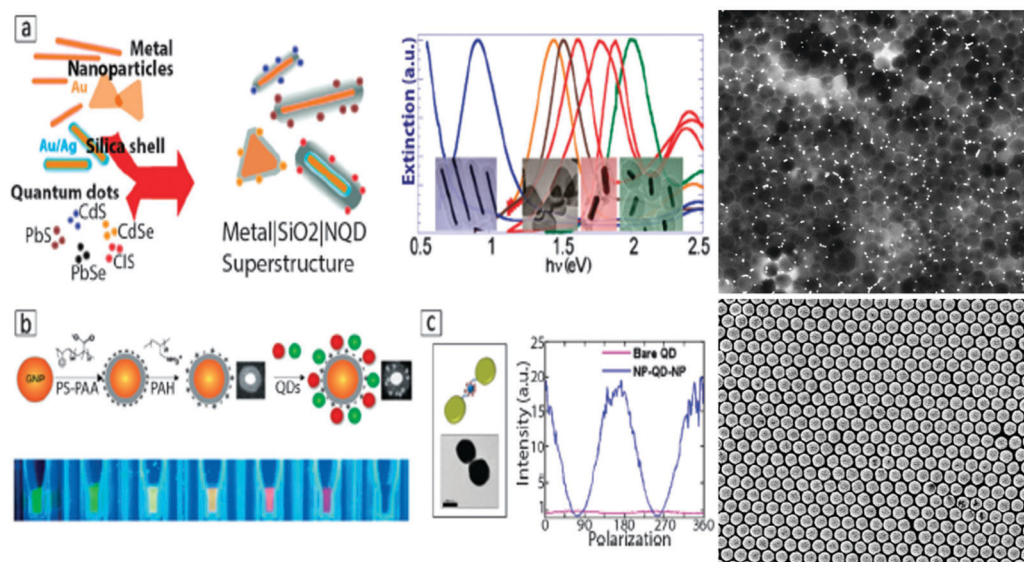This journal is © The Royal Society of Chemistry 2021

Fig. 6 Schematic representation of the self-assembly of hybrid metal nanostructures and silica spacer between metal NPs and Q-dots. Extinction spectra of hybrid metal nanostructures with different compositions.[94,96] Reproduced with permission from the Royal Society of Chemistry.[102]

have been conducted on the formation of pairs of colloid QDs, the size of obtainable pairs being much smaller than the wavelength of the inducing laser field wavelength.[100]

In Fig. 6, AuNPs are placed onto the 3D photonic crystal (3D-PC) based on PMMA nanostructures, which self-organize into the planes of superlattice. The binding of AuNPs onto the PMMA nanospheres is studied enormously in materials science due to a wide variety of optical and electronic properties. Polymer nanoparticles also exhibit some exclusive properties originating at nanoscale levels when quantum-confinement effects become dominant. AuNPs can be triggered to go through a self-organization process within 3D superlattices.[101,102] However, precise control over the wavelength scale is required to place the plasmonic materials in the crystal-lattice properly. The plasmonics of AuNPs has also been reported to increase the nonlinear response because of their strong interactions with the 3D-PCs.[103] In this way, the use of these nanoparticle assemblies may pave the way to tunable materials, in which colloidal size may control and change the optical and electronic properties. There is also another possibility. This may unlock the likelihood of merging 3D-PCs with plasmonics in a strong coupling regime as well as the improved confinement of robust plasmonic modes.[104]

5. Self-assembled plasmonic nanostructure-based applications

Sun *et al.* used augmented local field to study the well-ordered monolayer of Ag, as well as sandwiched nanostructures of Ag/SiO₂/Ag, incorporating layer-by-layer (LBL) film deposition and nanostructure self-assembly lithography (NSL) technique.[105] The isolated structures of connected nanospheres have been composed by precisely tuning the thickness of the sputtered film and size of polystyrene (PS) microspheres.[106–108] The improvement in SERS has been attributed to high LSPR of

isolated nanobowl structures (Fig. 7). The FDTD solution established the augmentation in the field to the SPR of interparticles over the Ag–SiO₂ interfaces.[109–111] The enhancement in SERS effects in Ag/SiO₂/Ag sandwiched nanobowl structures has been attributed chiefly to the SiO₂ layer by both experimental analysis and simulation results.

Furthermore, Sun *et al.* also successfully prepared ordered monolayer Ag nanobowl arrays and the Ag/SiO₂/Ag sandwich nano-bowl arrays over large-area, using LBL film deposition, combined with NSL technique. They also studied the variations in SERS properties, because of the construction and morphology of the nano-bowls. The plasmon coupling mechanism has also been investigated using the FDTD simulations at the interfaces of different materials for the nano-bowl structures.[111,112]

Modifications of the surfaces can tune the thin-film thickness and the polystyrene (PS) bead size. Strong SERS signals have been recorded, unlike the nano-hole-like arrangement and nano-bowl arrangement. The results have been attributed to SERS augmentation by the breaches between near-by PS and sharp edges. The strong SERS signals were also attributed to the plasma coupling at the gaps on the bottom of the bowl amid the inner and outer surface of the nanobowl structure and the Ag/SiO₂/Ag nanobowl assembly also verified the results.[113–115] The augmentation in both the charge-transfer and electromagnetic field has been attributed to SERS enhancement.[116,117]

5.1. Optoelectronic platforms

In 2013, Li and colleagues demonstrated a light-emitting diode (LED) platform with embedded PCs. In this work, the authors used nanosphere lithography (NSL) technique to create a close-packed array of nanopillars, which is embedded into an InGaN/GaN LED structure. The proposed nanopillar structure can provide light extraction and suppress the piezoelectric field through strain relaxation of the InGaN/GaN quantum wells at
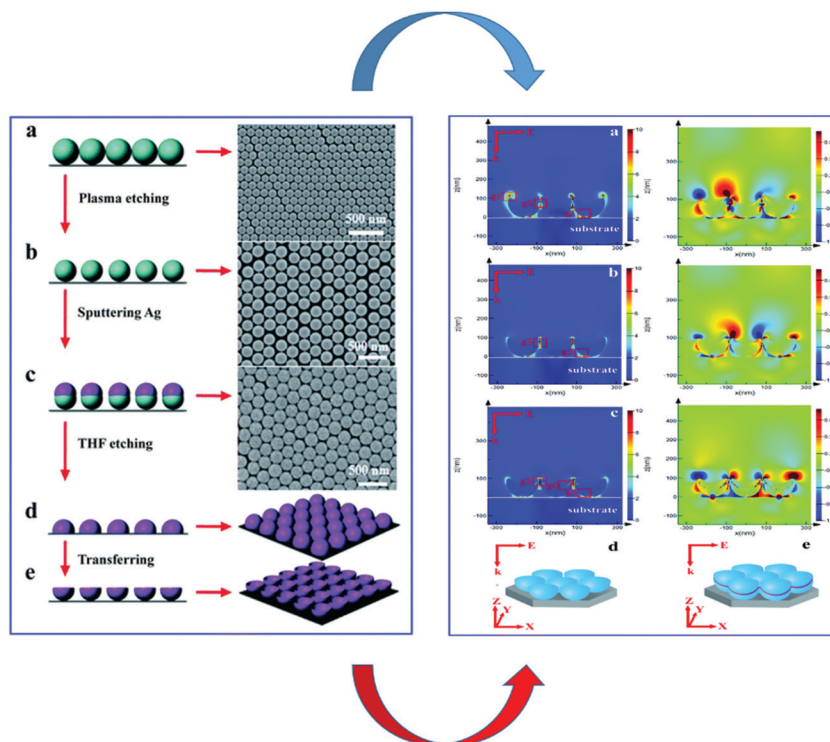
Fig. 7 Graphical diagram and the SEM micrographs of the fabrication method of silver nano-bowl and PS nanoparticles. The distribution of the electric field and charge-density for different nano-bowls excited by laser light of 514.5 nm. Reproduced with permission from the Royal Society of Chemistry.[106]

the same time. They reported that the LEDs with the embedded PCs can exhibit 20% more light than the considered reference LED. However, dye-synthesized solar cell (DSSC) concept is another way of producing photovoltaic devices, alternative to the conventional solid state semiconductor ones mainly due to their low cost of fabrication.

Zhang et al.[118] conducted theoretical investigations on the effect of the presence of a PC on the optical absorption of DSSCs (Fig. 8). To this end, a wavelength selective PC

concentrator DSSC has been developed. By overlapping the stop-band of the colloidal crystal films with the maximum fluorescence wavelength of the dye in the defect layer, a highly efficient laser feedback was obtained because of the photonic band gap effect of the colloidal crystal films. The low threshold lasing was realized through the confinement of radiated photons from the light-emitting layer in the laser-cavity structure. Besides, it showed the promise of the colloidal crystals as effective and selective reflection mirrors for lasers.
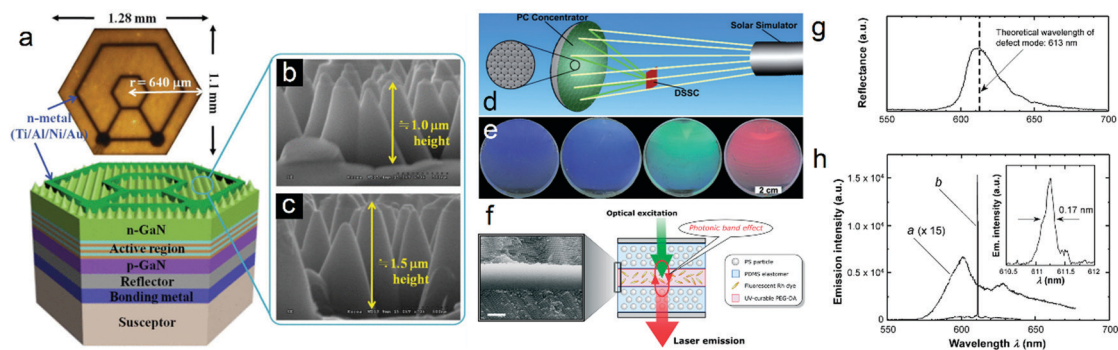

Fig. 8 (a) Top-view image (up) and schematic diagram of the proposed honey comb-type VLED chip. (b) Cross-sectional SEM images of the chip acquired at the n-GaN surface: (b) 1 μm-height and (c) 1.5 μm-height cone-shaped nanostructures. Adapted with permission from ref. 119. Copyright 2012 IEEE. (d) An illustration of the photovoltaic system with a PC concentrator. (e) Photographs of the PC concentrators with different stopbands: 448 nm, 475 nm, 530 nm, and 647 nm, respectively. Adapted with permission from Science Advances ref. 118. (f) A schematic exemplification of the developed colloidal crystal laser (CCL). A cross-sectional SEM image of the light-emitting planar defect is displayed on the left side. (g) The reflection spectrum of the CCL platform. Here, the dotted line points out the theoretical wavelength of the defect mode. (h) Emission spectra collected from the CCL device, resulting from optical excitation via the Nd:YAG laser beam with an energy of (a) 70 nJ per pulse and (b) 210 nJ per pulse. It is important to note that these spectra are magnified by 15 times. Inset: The zoom-in spectrum of the laser emission ~610 nm.

3376 | J. Mater. Chem. C, 2021, **9**, 3368–3383

This journal is © The Royal Society of Chemistry 2021

These achievements are some of the major steps towards low-threshold, ultra-lightweight, low-cost, and flexible light generation devices for opto-electronic applications.

5.2. Photonic crystals for 3D color printing

The 3D printers based on two-photon polymerization are incapable of patterning photonic crystal structures with the requisite ~300 nm lattice constant to achieve photonic stop-bands/bandgaps in the visible spectrum and generate colors. Here, we introduce a means to produce 3D-printed photonic crystals with a 5× reduction in lattice constants (periodicity as small as 280 nm), achieving sub-100 nm features with a full range of colors. The technology to print 3D structures in color on the microscopic scale promises the direct patterning and
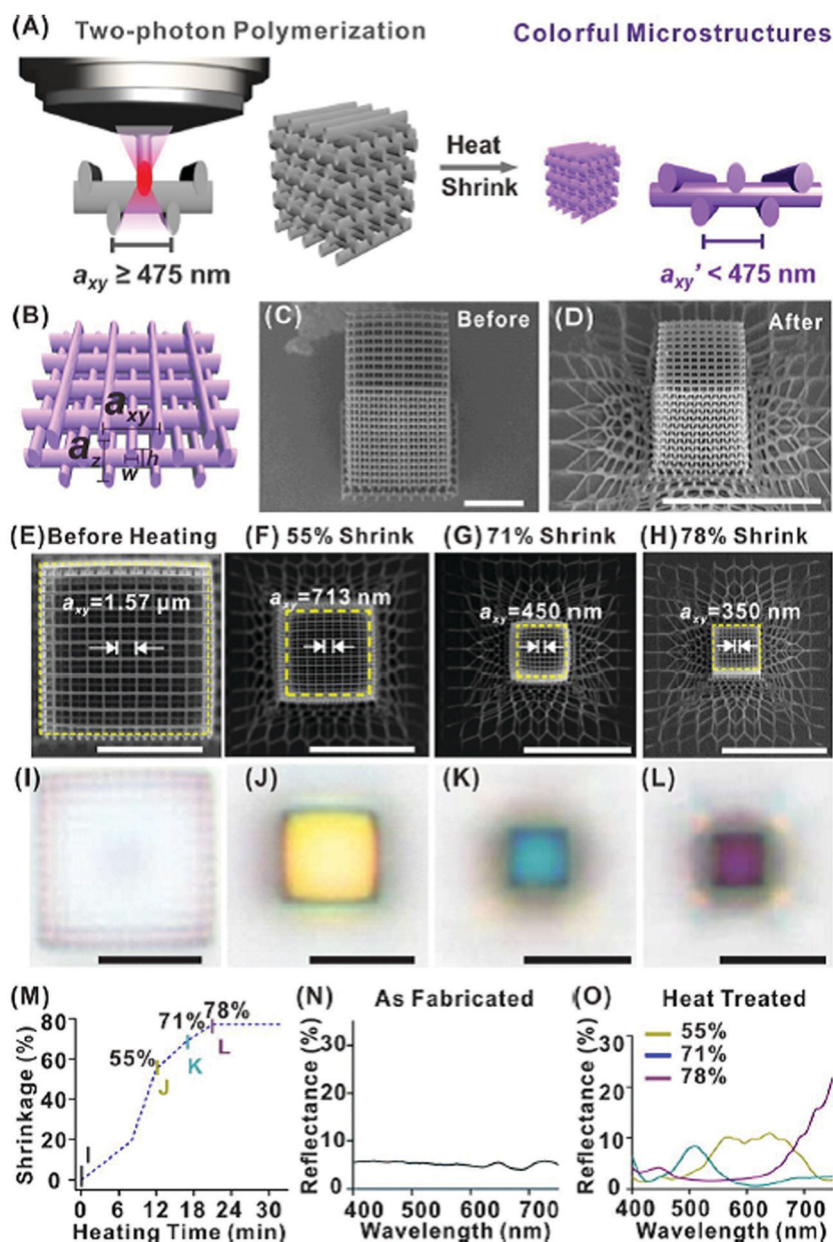

Fig. 9 Heat shrinking induced colors of 3D-printed woodpile photonic crystals. (A) Schematic of the fabrication process. Left: Woodpile photonic crystals written in commercial IP-Dip resist by two-photon polymerization at dimensions well above the resolution limit of the printer to prevent structures from collapsing. Right: After heat treatment, the dimensions of the photonic crystal are reduced below the resolution limit of the printer, and colors are generated. The colors change with different degrees of shrinkage. (B) Schematic showing one axial unit of the woodpile structure. axy and az denote the lateral and axial lattice constants, respectively. Tilted-view scanning electron micrographs (SEM) of a representative woodpile photonic crystal (C) before and (D) after heating. SEM images and the corresponding bright-field reflection-mode optical micrographs of the woodpile photonic crystal before heating (E and I) and with shrinkages of 55% (F and J), 71% (G and K), and 78% (H and L). (m) Shrinkage of the woodpile photonic crystal heated at ~450 °C as a function of heating duration. Reflectance spectra of the woodpile photonic crystal (N) before heating and (O) after heating with 55%, 71%, and 78% shrinkage. Scale bars represent 10 μm. Reproduced with permission from Elsevier Publication.[117]

This journal is © The Royal Society of Chemistry 2021

J. Mater. Chem. C, 2021, 9, 3368–3383 | 3377

integration of spectrally selective devices, such as photonic crystal-based color filters, onto free-form optical elements and curved surfaces.[116]

Fig. 9A introduces a shrinking method to enable the direct 3D printing of photonic crystals with stopbands in the visible range. Our approach combines the printing of 3D photonic structures using the Nanoscribe GmbH Photonic Professional GT and the IP-Dip resist, followed by a heat-induced shrinking process. To demonstrate the capability of this process, we fabricated woodpile photonic crystal structures with lattice constants as small as ∼280 nm, a dimension comparable to the finest periodicities in butterfly scales. The refractive index of the cross-linked polymer increases in the process, which is desirable for widening the stopbands for structural color applications.[120]

5.3. Photoelectrochemical water splitting using photonic crystals

Photoelectrochemical (PEC) water splitting is one of the most promising strategies to directly convert and store solar energy in the form of hydrogen. Searching for a kind of single- or multi-component photoelectrode material with high activity in the whole solar spectrum and currently long-term stability is still a challenge. Plasmonic metal nanostructures are the rising stars as photoactive materials due to their many exclusive properties such as high stability and extensively tunable optical response induced by surface plasmon resonance (SPR). In this work, an Au/TiO_2 composite photoelectrode was constructed by modifying Au nanoparticles (NPs) on a TiO_2 bi-layer structure with a bottom nanorod array layer and a top photonic crystal (PC) layer. By selectively tuning the slow-photon region of the TiO_2 PC by altering the structure parameters to match with the SPR region of Au NPs, a synergistically enhanced PEC water splitting efficiency was achieved.[121]

In order to compare the optical properties of TiO_2 NRs, Au/ TiO_2 NRs, TiO_2 NRPCs, and Au/TiO_2 NRPCs, diffused reflectance UV-Vis spectra were examined. The peak positions of the PGB of the TiO_2 NRPCs and the SPR of the Au NPs were closely connected to the dielectric constant of the surrounding media. Thus, all samples were completely filled with the electrolyte solution that was used for PEC characterization during the reflectance spectra measurements to obtain more realistic insights into the optical properties of these photoanodes. The optical reflectance of the TiO_2 NRs decreased sharply at a wavelength that was shorter than 415 nm (Fig. 10). In addition, slight absorption in the visible region was caused by undetectable light scattering and absorption of the FTO substrate, which were demonstrated to be negligible for the PEC water splitting processes.

6. Trends in plasmonics-based photonic device

Plasmonics is a science based on surface plasmon polaritons on metallic nano-structures. While this science has been established many years ago, it has again gained enthusiasm in the photonics community. This section of review explains the trends in plasmonics-based photonic devises according to Moore's law for integrated-circuits, as illustrated in Fig. 11. The discussion will be extended to the shape/size of nano-structures and the imaging ''beyond the plasmonics''.

As discussed in ref. 122 the interaction of non-monochromatic radiation with arrays comprising plasmonic and dielectric nanoparticles has been studied using the finite-difference time-domain electrodynamics method. It is shown that $LiNbO_3$, TiO_2, GaAs, Si, and Ge all-dielectric nanoparticle arrays can provide a complete selective reflection of an incident plane wave within a narrow spectral line of collective lattice resonance with a Q-factor of 10^3 or larger at various spectral ranges, while plasmonic refractory TiN and chemically stable Au nanoparticle arrays provide high-Q resonances with moderate reflectivity. Arrays with fixed dimensional parameters make it possible to
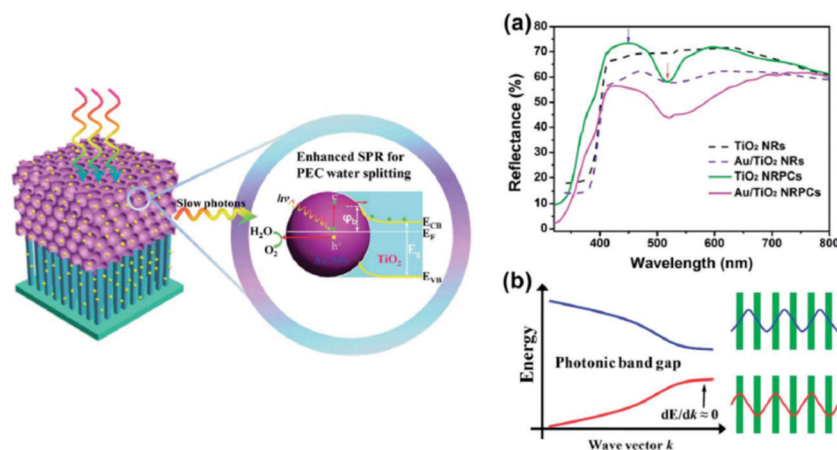

Fig. 10 (a) Diffused reflectance UV-Vis spectra of TiO_2 NRs, Au/TiO_2 NRs, TiO_2 NRPCs, and Au/TiO_2 NRPCs. All samples were prior filled with 1 M KOH aqueous solutions to ensure the same dielectric environment during the measurement processes. (b) Schematic optical band structure of PCs and electric field distributions of light near the blue edge and red edge of the photonic band gap. The green part indicates the high-dielectric region relative to the low-dielectric interval region. Reproduced with permission from Wiley Publications.[121]
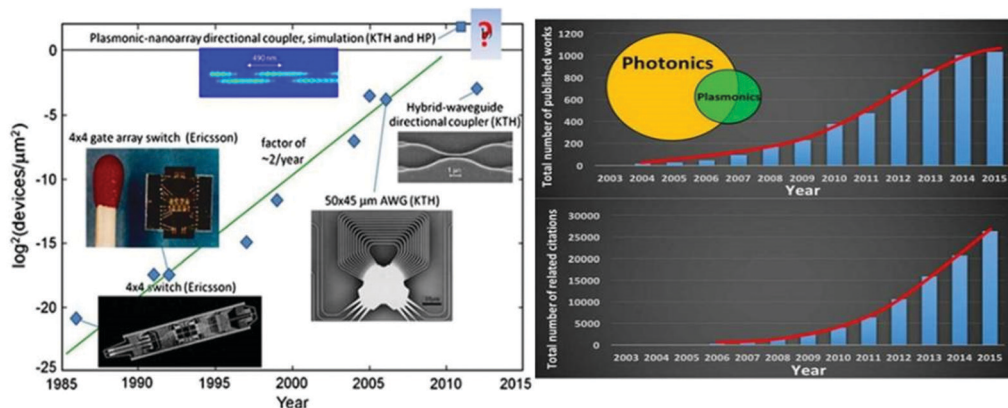
3378 | *J. Mater. Chem. C*, 2021, **9**, 3368–3383

This journal is © The Royal Society of Chemistry 2021

Fig. 11 Moore's law for integration density with respect to an equivalent number of components per square (μm) of integrated photonics devices, revealing rapid growth as compared to Moore's law for integrated-circuits, adapted from Thomson Reuters' Web of Science. The solid red lines are trend curves.

fine-tune the position of a selected resonant spectral line by tilting the array relative to the direction of the incident radiation. These effects provide grounds for engineering novel selective tunable optical high-Q filters in a wide range of wavelengths, from visible to middle-IR.

Collective lattice resonances (CLRs) in finite-size 2D arrays of dielectric nanospheres have been studied in ref. 123 *via* the coupled dipole approximation. We show that even for sufficiently large arrays, up to 100 nanoparticles (NPs), electric or magnetic dipole CLRs may significantly differ from the ones calculated for infinite arrays with the same geometrical properties (NP sizes and interparticle distances). The discrepancy is explained with the existence of a sufficiently strong cross-interaction between electric and magnetic dipoles induced at NPs in finite-size lattices, which is ignored for infinite arrays. This claim was supported numerically, as well as an analytic model to estimate a spectral width of CLRs for finite-size arrays has been proposed. Provided that the current theoretical and numerical research on collective effects in arrays of dielectric NPs mostly rely on modeling infinite structures, the findings may contribute to thoughtful and optimal design of inherently finite-size photonic devices.

Collective lattice resonances in disordered 2D arrays of spherical Si nanoparticles (NPs) have been thoroughly studied in ref. 124 and 127 within the framework of the coupled dipole approximation. Three types of defects have been analyzed: positional disorder, size disorder, and quasi-random disorder. It was shown that the positional disorder strongly suppresses either the electric dipole (ED) or the magnetic dipole (MD) coupling depending on the axis along which the NPs are shifted. On the contrary, size disorder strongly affects only the MD response, while the ED resonance can be almost intact, depending on the lattice configuration. Finally, random removing of NPs from an ordered 2D lattice reveals a quite surprising result: hybridization of the ED and MD resonances with lattice modes remains observable even in the case of random removing of up to 84% of the NPs from the ordered array. Reported results could be important for rational design and utilization of metasurfaces, solar cells and other all-dielectric photonic devices.

As explained in ref. 125 and 128, authors analytically and numerically studied coupling mechanisms between the 1D photonic crystal (PhC) and 2D array of plasmonic nanoparticles (NPs) embedded in its defect layer. Authors introduced general formalism to explain and predict the emergence of PC-mediated Wood–Rayleigh anomalies, whose spectral positions agreed well with the results of exact simulations by the finite-difference time-domain (FDTD) method. Electromagnetic coupling between localized surface plasmon resonance (LSPR) and PC-mediated Wood–Rayleigh anomalies makes it possible to efficiently tailor PhC modes.[129] The understanding of coupling mechanisms in such a hybrid system paves a way for optimal design of sensors, light absorbers, modulators and other types of modern photonic devices with controllable optical properties.

Authors of the research article as ref. 126, 130 and 131 studied thermal effects occurring during excitation of optical plasmonic waveguide (OPW) in the form of linear chain of spherical Ag nanoparticles by pulsed laser radiation. It was shown that heating and subsequent melting of the first irradiated particle in a chain can significantly deteriorate the transmission efficiency of OPW that is the crucial and limiting factor, and continuous operation of OPW requires cooling devices. This effect is caused by suppression of particle's surface plasmon resonance due to reaching the melting point temperature. We have determined optimal excitation parameters, which do not significantly affect the transmission efficiency of OPW.

7. Challenges and viewpoint

The research opportunity for nanostructured plasmonic photonic materials having periodic nanostructures has swiftly extended to conventional complex nanostructures for their versatile use in optical devices, as illustrated in Fig. 12. The rapid technological advancements are expected to further improve the photonic viability of composite substances, better control over structural imperfections, and the integration of optical gadgets in the near future. Synthesizing the plasmonic nanomaterials having desired optical and electronic characteristics while keeping high RI,
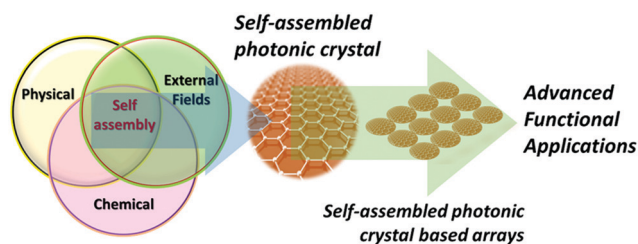
This journal is © The Royal Society of Chemistry 2021

J. Mater. Chem. C, 2021, **9**, 3368–3383 | **3379**

Fig. 12 Collective approach of materials science to develop self-assembled photonic crystals for advanced applications.

creations of materials with further versatile sensing functionalities and optical-active hybrid plasmonic photonic nanostructured substances is critically required for the progress of plasmonic photonic nanostructured materials. For the successful industrialization of photonic polymer materials, some essential norms may be the explicit feasibility of polymers, fast dynamic reaction to specific, and/or various, external stimulating signals. Plasmonic photonic nanostructures may also prove their tremendous contribution to a highly increasing demand for further protection of ultra-secure data storage devices such as credit/debit cards and identification documents.

The plasmonic photonic nanostructures may perform tremendously vital characters in prospective polymer recording media with enhanced multiple security aspects and can provide low-cost optical modules to read, write, and scan. However, control of the traps and defects in periodic structures, while fabricating large-scale self-assemblies of almost-perfect crystalline structures is a whole good deal of struggles. The self-assembly technique is a relatively cost-effective approach to fabricate PCCs of polymers for the use in photonic sensing, which requires defect-tolerant materials and can be deposited onto the substrates of arbitrary patterns. Among the several benefits of micro-fabricated polymer systems, precise control over the final pattern, introduction of predefined features and symmetries in PPCs using the latest expertise and sophisticated instruments are worth mentioning. However, the costly techniques for microfabrication with a relatively less output are the main problem. Antireflective coating, ultra-precise optical filter, super-prism and PC-fiber optics are just some of the versatile applications of PPCs. The combination of electron-beam lithography with holography and two-photon polymerization with self-assembled structures and some other sophisticated techniques may be used to prevent the formation of defects in 3-DD PPCs.

The integration of PPC devices with different optoelectronic modules and the coupling with optical waveguides is the present challenge in this area of research. The fabrication of PPCs by precisely tailoring the shape, size, optical, mechanical and thermal properties is still a great challenge and once solved, it will pave the way to incorporate features like having ultra-low energy consumption, broad communication-bandwidth, ultra-fast optical computing and lasing for future gadgets.

Conflicts of interest

Authors declare no conflict of interest.

References

1 E. Yablonovitch, *Phys. Rev. Lett.*, 1987, **58**, 2059.
2 S. John, *Phys. Rev. Lett.*, 1987, **58**, 2486.
3 E. L. Hu, M. Brongersma and A. Baca, *Applications: Nanophotonics and Plasmonics. In Nanotechnology Research Directions for Societal Needs in 2020*, Springer, Dordrecht, The Netherlands, 2008, pp. 318–340.
4 J. F. Galisteo-Lõpez, M. Ibisate, R. Sapienza, L. S. Froufe-Pérez, Ú. Blanco and C. Lõpez, Self-assembled photonic structures, *Adv. Mater.*, 2011, **23**, 30–69.
5 R. Amria, S. Sahela, D. Gamra, M. Lejeune, M. Clin, K. Zellama and H. Bouchrih, *Superlattices Microstruct.*, 2017, **104**, 298–307.
6 M. I. Stockman, *Phys. Today*, 2011, **64**, 39–44.
7 M. Moskovits, in *Near-field optics and surface plasmon polaritons*, ed. S. Kawata, Springer, Berlin, 2001.
8 Y. Zakharko, T. Nychyporuk, L. Bonacina, M. Lemiti and V. Lysenko, *Nanotechnology*, 2013, **24**, 055703.
9 W. Zhou, M. Dridi, J. Y. Suh, C. H. Kim, D. T. Co, M. R. Wasielewski, G. C. Schatz and T. W. Odom, *Nat. Nanotechnol.*, 2013, **8**, 506–511.
10 D. B. Shao and S. C. Chen, *Appl. Phys. Lett.*, 2005, **86**, 253107.
11 F. Li, D. P. Josephson and A. Stein, Colloidal assembly: The road from particles to colloidal molecules and crystals, *Angew. Chem., Int. Ed.*, 2011, **50**, 360–388.
12 D. J. de Aberasturi, A. B. Serrano-Montes and L. M. Liz-Marzán, *Adv. Opt. Mater.*, 2015, **3**(5), 602–617.
13 C.-F. Lai, 2016, Book chapter published by INECH, DOI: 10.5772/65007.
14 D. J. Norris, E. G. Arlinghaus, L. Meng, R. Heiny and L. Scriven, *Adv. Mater.*, 2004, **16**, 1393–1399.
15 J.-N. Liu, Q. Huang, K.-K. Liu, S. Singamaneni and B. T. Cunningham, *Nano Lett.*, 2017, **17**, 7569–7577.
16 H. Chen, L. Shao, Q. Li and J. Wang, *Chem. Soc. Rev.*, 2013, **42**, 2679–2724.
17 M. L. Garcìa, *Self-Assembled Photonic-Plasmonic Crystals for Light control at the Nanoscale*, PhD thesis, Universidade de Santiago de Compostela (España) en, 2011.
18 J. Xaviera, S. Vincenta, F. Medera and F. Vollmera, Advances in optoplasmonic sensors – combining optical nano/microcavities and photonic crystals with plasmonic nanostructures and nanoparticles, *Nanophotonics*, 2018, **7**(1), 1–38.
19 E. Cohen-Hoshen, G. W. Bryant, I. Pinkas, J. Sperling and I. Bar-Joseph, *Nano Lett.*, 2012, **12**, 4260–4264.

3380 | *J. Mater. Chem. C*, 2021, **9**, 3368–3383

This journal is © The Royal Society of Chemistry 2021

20 M. Yang, G. Chen, Y. Zhao, G. Silber, Y. Wang, S. Xing, Y. Han and H. Chen, *Phys. Chem. Chem. Phys.*, 2010, **12**, 11850–11860.

21 D. Nykypanchuk, M. M. Maye, D. van der Lelie and O. Gang, *Nature*, 2008, **451**, 549–552.

22 J. Govan and Y. K. Gun'ko, Recent progress in chiral inorganic nanostructures, *Nanoscience*, 2016, **3**, 1–30.

23 P. P. Patra, R. Chikkaraddy, R. P. N. Tripathi, A. Dasgupta and G. V. P. Kumar, Plasmofluidic single-molecule surface-enhanced Raman scattering from dynamic assembly of plasmonic nanoparticles, *Nat. Commun.*, 2014, **5**, 4357.

24 S. Kasera, F. Biedermann, J. J. Baumberg, O. A. Scherman and S. Mahajan, Quantitative SERS using the sequestration of small molecules inside precise plasmonic nanoconstructs, *Nano Lett.*, 2012, **12**, 5924–5928.

25 S. S. Acimovic, M. A. Ortega and V. Sanz, *et al.*, LSPR chip for parallel, rapid, and sensitive detection of cancer markers in serum, *Nano Lett.*, 2014, **14**, 2636–2641.

26 E. Bermúdez-Ureña, G. Tutuncuoglu and J. Cuerda, *et al.*, Plasmonic waveguide-integrated nanowire laser, *Nano Lett.*, 2017, **17**, 747–754.

27 A. Yadav, M. Danesh, L. Zhong, G. J. Cheng, L. Jiang and L. Chi, *Nanotechnology*, 2016, **27**(16), 165703.

28 A. Yadav, L. Zhong, J. Sun, L. Jiang, G. J. Cheng and L. Chi, *Nano Convergence*, 2017, **4**(1), 1.

29 H. Gu, Y. Zhao, Y. Cheng, Z. Xie, F. Rong, J. Li, B. Wang, D. Fu and Z. Gu, *Small*, 2013, **9**, 2266.

30 X. Su, J. Jiang, X. Sun, S. Wu, B. Tang, W. Niu and S. Zhang, *Nanoscale*, 2017, **9**, 17877.

31 S.-T. Wu and A. Ying-GueyFuh, *Jpn. J. Appl. Phys.*, 2005, **44**(1), 2.

32 D. Budaszewski, M. Chychłowski, A. Budaszewska, B. Bartosewicz, B. Jankiewicz and T. R. Woliński, *Opt. Express*, 2019, **27**(10), 14260–14269.

33 P. S. J. Russell, Photonic-Crystal Fibers, *J. Lightwave Technol.*, 2006, **24**(12), 4729–4749.

34 T. T. Larsen, A. Bjarklev and D. S. Hermann, Optical devices based on liquid crystal photonic bandgap fibres 2003, **11**(20), 2589–2596.

35 T. R. Woliński, K. Szaniawska, K. Bondarczuk, P. Lesiak and A. W. Domański, Propagation properties of photonic crystal fibers filled with nematic liquid crystals, *Opto-Electron. Rev.*, 2005, **13**(2), 177–182.

36 L. Scolari, S. Gauza, H. Xianyu, L. Zhai, L. Eskildsen, T. T. Alkeskjold, S.-T. Wu and A. Bjarklev, Frequency tunability of solid-core photonic crystal fibers filled with nanoparticle-doped liquid crystals, *Opt. Express*, 2009, **17**(5), 3754–3764.

37 S. Pillai, K. R. Catchpole, T. Trupke and M. A. Green, *J. Appl. Phys.*, 2007, **101**, 093105.

38 H. Cong, B. Yu, J. Tang, Z. Li and X. Liu, Current status and future developments in preparation and application of colloidal crystals, *Chem. Soc. Rev.*, 2013, **42**, 7774–7800.

39 J. F. Galisteo-Lôpez, M. Ibisate, R. Sapienza, L. S. Froufe-Pérez, Ú. Blanco and C. Lõpez, Self-assembled photonic structures, *Adv. Mater.*, 2011, **23**, 30–69.

40 J. Ge and Y. Yin, Responsive photonic crystals, *Angew. Chem., Int. Ed.*, 2011, **50**, 1492–1522.

41 S.-H. Kim, S. Y. Lee, S.-M. Yang and G.-R. Yi, Self-assembled colloidal structures for photonics, *NPG Asia Mater.*, 2011, **3**, 25–33.

42 V. A. Ignatchenko and D. S. Tsikalov, *Phys. Proc.*, 2017, **86**, 113–116.

43 A. B. D. Nandiyanto, T. Ogi, F. Iskandar and K. Okuyama, *Chem. Eng. J.*, 2011, **167**, 409–415.

44 P. Jiang and M. J. McFarland, *J. Am. Chem. Soc.*, 2004, **126**, 13778–13786.

45 Y.-H. Ye, T. S. Mayer, I.-C. Khoo, I. B. Divliansky, N. Abrams and T. E. Mallouk, *J. Mater. Chem.*, 2002, **12**, 3637–3639.

46 C.-F. Lai, Colloidal photonic crystals containing copper-oxide and silver nanoparticles with tunable structural colors, *Advances in Colloid Science*, IntechOpen, 2016.

47 T. Ding, K. Song, K. Clays and C.-H. Tung, *Langmuir*, 2010, **26**(6), 4535–4539.

48 G. v. Freymann, V. Kitaev, B. V. Lotsch and G. A. Ozin, *Chem. Soc. Rev.*, 2013, **42**(7), 2528–2554.

49 A. R. Tao, J. Huang and P. Yang, *Acc. Chem. Res.*, 2008, **41**(12), 1662–1673.

50 S. Fazal, J. Aswathy, S. Sasidharan and D. Menon, *ACS Appl. Mater. Interfaces*, 2014, **6**, 11.

51 T. Watanabe, Y. Saijo, Y. Hasegawa, K. Watanabe, Y. Nishijima and T. Baba, *Opt. Express*, 2017, **25**(20), 24469.

52 S.-J. Ko, H. Choi, W. Lee, T. Kim, B. R. Lee, J.-W. Jung, J.-R. Jeong, M. H. Song, J. C. Lee, H. Y. Woo and J. Y. Kim, Highly Efficient Plasmonic Organic Optoelectronic Devices Based on a Conducting Polymer Electrode Incorporated with Silver Nanoparticles, *Energy Environ. Sci.*, 2013, **6**, 1949–1955.

53 V. Jankovic, Y. Yang, J. You, L. Dou, Y. Liu, P. Cheung, J. P. Chang and Y. Yang, Active Layer-Incorporated, Spectrally Tuned Au/SiO2 Core/Shell Nanorod-Based Light Trapping for Organic Photovoltaics, *ACS Nano*, 2013, **7**, 3815–3822.

54 R. Mayoral, J. Requena, J. S. Moya, C. Lòpez, A. Cintas, H. Míguez, F. Meseguer, L. Vázquez, M. Holgado and A. Blunco, *Adv. Mater.*, 1997, **9**, 257.

55 G. Widawski, M. Rawiso and B. Francois, *Nature*, 1994, **369**, 387.

56 A. R. Parker and Y. Xia, *Adv. Mater.*, 1998, **10**, 1045.

57 A. S. Dimitrov and K. Nagayama, *Langmuir*, 1996, **12**, 1303.

58 P. Jiang, J. F. Bertone, K. S. Hwang and V. L. Colvin, *Chem. Mater.*, 1999, **11**, 2132.

59 S. M. Yang, H. Míguez and G. A. Ozin, *Adv. Funct. Mater.*, 2002, **12**, 425.

60 Y. A. Vlasov, X. Z. Bo, J. C. Sturm and D. J. Norris, *Nature*, 2001, **414**, 289.

61 Z. Gu, A. Fujishima and O. Sato, *Chem. Mater.*, 2002, **14**, 760.

62 P. Liu, L. Bai, J. Yang, H. Gu, Q. Zhong, Z. Xie and Z. Gu, Self-assembled colloidal arrays for structural color, *Nanoscale Adv.*, 2019, **1**, 1672.

63 L. Woodcock, *Nature*, 1997, **385**, 141.

This journal is © The Royal Society of Chemistry 2021

J. Mater. Chem. C, 2021, **9**, 3368–3383 | **3381**

64 Z. Gu, Q. Meng, S. Hayami, A. Fujishima and O. Sato, *J. Appl. Phys.*, 2001, **90**, 2042.

65 A. V. Blaaderen, R. Ruel and P. Wiltzius, *Nature*, 1997, **385**, 321.

66 P. V. Braun, R. W. Zehner, C. A. White, M. K. Weldon, C. Kloc, S. S. Patel and P. Wiltzius, *Adv. Mater.*, 2001, **13**, 721.

67 S. M. Yang, H. Míguez and G. A. Ozin, *Adv. Funct. Mater.*, 2002, **12**, 425.

68 S. H. Kim, S. J. Jeon, G. R. Yi, C. J. Heo, J. H. Choi and S. M. Yang, *Adv. Mater.*, 2008, **20**, 1649.

69 S. H. Kim, S. J. Jeon, W. C. Jeong, H. S. Park and S. M. Yang, *Adv. Mater.*, 2008, **20**, 4129.

70 J. J. Bohn, M. Ben-Moshe, A. Tikhonov, D. Qu, D. N. Lamont and S. A. Asher, *J. Colloid Interface Sci.*, 2010, **344**, 298.

71 J. E. Aw, G. T. W. Goh, S. Huang, M. R. Reithofer, A. Z. Thong and J. M. Chin, *Langmuir*, 2015, **31**, 6688.

72 Z. Chen, M. Mo, F. Fu, L. Shang, H. Wang, C. Liu and Y. Zhao, *ACS Appl. Mater. Interfaces*, 2017, **9**, 38901.

73 S. Noda, M. Fujita and T. Asano, *Nat. Photonics*, 2007, **1**, 449.

74 Z. Yin, Y. S. Zhu, W. Xu, J. Wang, S. Xu, B. Dong, L. Xu, S. Zhang and H. W. Song, *Chem. Commun.*, 2013, **49**, 3781.

75 B. Y. Ding, C. Hrelescu, N. Arnold, G. Isic and T. A. Klar, *Nano Lett.*, 2013, **13**, 378.

76 Z. Yin, H. Li, W. Xu, S. Cui, D. Zhou, X. Chen, Y. Zhu, G. Qin and H. Song, Local Field Modulation Induced Three-Order Upconversion Enhancement: Combining Surface Plasmon Effect and Photonic Crystal Effect, *Adv. Mater.*, 2016, **28**, 13.

77 X. Liu and D. Y. Lei, *Sci. Rep.*, 2015, **5**, 15235.

78 C. J. Murphy, T. K. San, A. M. Gole, C. J. Orendorff, J. X. Gao, L. Gou, S. E. Hunyadi and T. Li, *J. Phys. Chem. B*, 2005, **109**, 13857.

79 X. Ye, C. Zheng, J. Chen, Y. Gao and C. B. Murray, *Nano Lett.*, 2013, **13**, 765.

80 Q. Liu, W. Feng, T. S. Yang, T. Yi and F. Y. Li, *Nat. Protoc.*, 2013, **8**, 2033.

81 G. B. Shan and G. P. Demopoulos, *Adv. Mater.*, 2010, **22**, 4373.

82 J. Lee, P. W. Bisso, R. L. Srinivas, J. J. Kim, A. J. Swiston and P. S. Doyle, *Nat. Mater.*, 2014, **5**, 524.

83 C. Wurth, M. Grabolle, J. Pauli, M. Spieles and U. Resch-Genger, *Nat. Photonics*, 2013, **8**, 1535.

84 V. Bliznyuk, S. Singamaneni, S. Sahoo, S. Polisetty, X. He and C. Binek, *Nanotechnology*, 2009, **20**, 105606.

85 L. N. Kim, E.-G. Kim, J. Kim, S.-E. Choi, W. Park and S. Kwon, *Bull. Korean Chem. Soc.*, 2012, **33**, 3735–3739.

86 M. Motornov, S. Z. Malynych, D. S. Pippalla, B. Zdyrko, H. Royter, Y. Roiter, M. Kahabka, A. Tokarev, I. Tokarev, E. Zhulina, K. G. Kornev, I. Luzinov and S. Minko, *Nano Lett.*, 2012, **12**, 3814–3820.

87 J. Henzie, S. C. Andrews, X. Yi, Z. Li and P. Yang, *Proc. Natl. Acad. Sci. U. S. A.*, 2013, **110**, 6640–6645.

88 M. Rycenga, P. H. C. Camargo and Y. Xia, *Soft Matter*, 2009, **5**, 1129–1136.

89 S. J. Tan, M. J. Campolongo, D. Luo and W. Cheng, *Nat. Nanotechnol.*, 2011, **6**, 268–276.

90 P. S. Kuo, J. Bravo-Abad and G. S. Solomon, Second-harmonic generation using -quasi-phasematching in a GaAs whispering-gallery-mode microcavity, *Nat. Commun.*, 2014, **5**, 3109.

91 B. Khanaliloo, M. Mitchell, A. C. Hryciw and P. E. Barclay, High-Q/V monolithic diamond microdisks fabricated with quasi-isotropric etching, *Nano Lett.*, 2015, **15**, 5131–5136.

92 R. Chen, S. Gupta and Y. C. Huang, *et al.*, Demonstration of a Ge/GeSn/Ge quantum-well microdisk resonator on silicon:enablinghighqualityGeSn; materials for micro- and nanophotonics, *Nano Lett.*, 2013, **14**, 37–43.

93 V. V. Slabko, G. G. Khachatryan and A. S. Aleksandrovsky, Self-organized aggregation of small metal particles controlled by an external light field, *JETP Lett.*, 2006, **84**, 300.

94 J. T. Lin, Y. X. Xu and Z. W. Fang, *et al.*, Fabrication of high-Q lithium niobate microresonators using femtosecond laser micromachining, *Sci. Rep.*, 2015, **5**, 8072.

95 M. I. Stockman, *Phys. Today*, 2011, **64**, 39–44.

96 M. Dasog, G. B. De los Reyes, L. V. Titova, F. A. Hegmann and J. G. C. Veinot, Size *vs* Surface: Tuning the Photoluminescence of Freestanding Silicon Nanocrystals Across the Visible Spectrum *via* Surface Groups, *ACS Nano*, 2014, **8**, 9979.

97 A. W. Achtstein, A. Schliwa, A. Prudnikau, M. Hardzei, M. V. Artemyev, C. Thomsen and U. Woggon, Electronic Structure and Exciton–Phonon Interaction in Two-Dimensional Colloidal CdSe Nanosheets, *Nano Lett.*, 2012, **12**, 5756.

98 P. M. Bendix, L. Jauffred, K. Norregaard and L. B. Oddershede, Optical Trapping of Nanoparticles and Quantum Dots, *IEEE J. Sel. Top. Quantum Electron.*, 2014, **20**(3), 4800112.

99 V. V. Slabko, A. S. Tsipotan and A. S. Aleksandrovsky, Resonant light-controlled self-assembly of ordered nanostructures, *Opt. Express*, 2012, **10**, 636.

100 A. S. Tsipotan, M. A. Gerasimova, V. V. Slabko and A. S. Aleksandrovsky, Laser-induced wavelength-controlled self-assembly of colloidal quasi-resonant quantum dots, *Opt. Express*, 2016, **24**, 11145.

101 L. Deng, L. Liu, C. Zhu, D. Li and S. Dong, *Chem. Commun.*, 2013, **49**, 2503–2505.

102 A. Klinkova, R. M. Choueiri and E. Kumacheva, Self-assembled plasmonic nanostructures, *Chem. Soc. Rev.*, 2014, 3976–3991.

103 A. Yadav, S. Elshahat, L. Bibbò, K. Khan, X. Tang, J. Prakash, G. J. Cheng, A. Kaushik and Z. Ouyang, Fabrication of self-assembled three-dimensional nano-photonic crystals and potential applications, *Sci. Adv. Today*, 2017, **3**, 25275.

104 R. L. Whetten, *et al.*, *Adv. Mater.*, 1996, **8**, 428–433.

105 D. Genov, R. Oulton, G. Bartal and X. A. Zhang, *Phys. Rev. B: Condens. Matter Mater. Phys.*, 2011, **83**, 245312.

106 H. Sun, L. Chen, Y. Wang, Z. Hua, Y. Liu, Y. Zhang and J. Yang, Increasing local field by interfacial coupling in nanobowl arrays, *RSC Adv.*, 2017, 69.

3382 | *J. Mater. Chem. C*, 2021, **9**, 3368–3383

This journal is © The Royal Society of Chemistry 2021

107 Y. X. Wang, X. Y. Zhao, L. Chen, S. Chen, M. B. Wei, M. Gao, Y. Zhao, C. Wang, X. Qu, Y. J. Zhang and J. H. Yang, Ordered nanocap array composed of SiO$_2$-isolated Ag islands as SERS platform, *Langmuir*, 2014, **30**, 15285–15291.

108 K. Chen, B. B. Rajeeva, Z. L. Wu, M. Rukavina, T. D. Dao, S. Ishii, M. Aono, T. Nagao and Y. B. Zheng, Moirénanosphere lithography, *ACS Nano*, 2015, **9**, 6031–6040.

109 J. Yu, C. Geng, L. Zheng, Z. H. Ma, T. Y. Tan, X. Q. Wang, Q. F. Yan and D. Z. Shen, Preparation of high-quality colloidal mask for nanosphere lithography by a combination of air/water interface self-assembly and solvent vapor annealing, *Langmuir*, 2012, **28**, 12681–12689.

110 W. B. Cai, B. Ren, X. Q. Li, C. X. She, F. M. Liu, X. W. Cai and Z. Q. Tian, Investigation of surface-enhanced Raman scattering from platinum electrodes using a confocal Raman microscope: dependence of surface roughening pretreatment, *Surf. Sci.*, 1998, **406**, 9–22.

111 M. Frederiksen, V. E. Bochenkov, M. B. Cortie and D. S. Sutherland, Plasmon hybridization and field confinement in multilayer metal–dielectric nanocups, *J. Phys. Chem. C*, 2013, **117**, 15782–15789.

112 J. Lee, Q. P. Zhang, S. Y. Park, A. Choe, Z. Y. Fan and H. Ko, Particle–film plasmons on periodic silver film over nanosphere (AgFON): a hybrid plasmonic nanoarchitecture for surface-enhanced Raman spectroscopy, *ACS Appl. Mater. Interfaces*, 2015, **8**, 634–642.

113 F. F. Wen, J. Ye, N. Liu, P. V. Dorpe, P. Nordlander and N. J. Halas, Plasmon transmutation: inducing new modes in nanoclusters by adding dielectric nanoparticles, *Nano Lett.*, 2012, **12**, 5020–5026.

114 Y. Liu, H. Wang, J. Ho, R. C. Ng, R. J. H. Ng, V. H. Hall-Chen, E. H. H. Koay, Z. Dong, H. Liu, C. W. Qiu, J. R. Greer and J. K. W. Yang, Structural color three-dimensional printing by shrinking photonic crystals, *Nat. Commun.*, 2019, **10**(1), 4340.

115 D. D. Lin, Z. L. Wu, S. J. Li, W. Q. Zhao, C. J. Ma, J. Wang, Z. M. Jiang, Z. Y. Zhong, Y. B. Zheng and X. J. Yang, Large-Area Au-Nanoparticle-Functionalized Si Nanorod Arrays for Spatially Uniform Surface-Enhanced Raman Spectroscopy, *ACS Nano*, 2017, **11**, 1478–1487.

116 L. Chen, H. H. Sun, Y. Zhao, R. X. Gao, Y. X. Wang, Y. Liu, Y. J. Zhang, Z. Hua and J. H. Yang, Iron Layer-Dependent Surface-Enhanced Raman Scattering of Hierarchical Nanocap Arrays, *Appl. Surf. Sci.*, 2017, **423**, 1124–1133.

117 Y. J. Zhang, C. Wang, J. Wang, J. P. Wang, L. Chen, J. Li, Y. Liu, X. Y. Zhao, Y. X. Wang and J. H. Yang, Nanocap array of Au: Ag composite for surface-enhanced Raman scattering, *Spectrochim. Acta, Part A*, 2016, **152**, 461–467.

118 L. Chen, Y. Zhao, Y. J. Zhang, M. M. Liu, Y. X. Wang, X. Qu, L. Yang, J. Li, X. Y. Liu and J. H. Yang, Design of Cu2O-Au composite microstructures for surface-enhanced Raman scattering study, *Colloids Surf., A*, 2016, **507**, 96–102.

119 A. Yadav, S. Elshahat, L. Bibbò, K. Khan, X. Tang, J. Prakash, G. J. Cheng, A. Kaushik and Z. Ouyang, Fabrication of self-assembled three-dimensional nano-photonic crystals and potential applications, *Sci. Adv. Today*, 2017, **3**, 25275.

120 L. Chen, H. H. Sun, Y. Zhao, Y. J. Zhang, Y. X. Wang, L. Yang, X. L. Zhang, Y. H. Jiang, Z. Hua and J. H. Yang, Plasmonic induced SERS enhancement of shell-dependent Ag@Cu$_2$O core-shell nanoparticles, *RSC Adv.*, 2017, **7**, 16553–16560.

121 G. Collins, E. Armstrong, D. McNulty, S. O'Hanlon, H. Geaney and C. O'Dwyer, 2D and 3D photonic crystal materials for photocatalysis and electrochemical energy storage and conversion, *Sci. Technol. Adv. Mater.*, 2016, **17**(1), 563–582.

122 D. Utyushev, I. L. Isaev, V. S. Gerasimov, A. E. Ershov, V. I. Zakomirnyi, I. L. Rasskazov, S. P. Polyutov, H. Ågren and S. V. Karpov, *Opt. Express*, 2020, **28**(2), 1426–1438.

123 V. I. Zakomirnyi, A. E. Ershov, V. S. Gerasimov, S. V. Karpov, H. Ågren and I. L. Rasskazov, Collective lattice resonances in arrays of dielectric nanoparticles: a matter of size, *Opt. Lett.*, 2019, **44**(23), 5743–5746.

124 V. I. Zakomirnyi, S. V. Karpov, H. Agren and I. L. Rasskazov, Collective lattice resonances in disordered and quasi-random all-dielectric metasurfaces, *J. Opt. Soc. Am. B*, 2019, **36**(7), E21–E29.

125 V. S. Gerasimov, A. E. Ershov, R. G. Bikbaev, I. L. Rasskazov, I. V. Timoifeev, S. P. Polyutov and S. V. Karpov, Engineering Mode Hybridization in Regular Arrays of Plasmonic Nanoparticles Embedded in 1D Photonic Crystal, *J. Quant. Spectrosc. Radiat. Transfer*, 2019, **224**, 303–308.

126 V. I. Zakomirnyi, V. S. Gerasimov, A. E. Ershov, I. L. Rasskazov, A. P. Gavrilyuk, S. V. Karpov and A. P. Polyutov, Thermal limiting effects in optical plasmonic waveguides, *J. Quant. Spectrosc. Radiat. Transfer*, 2017, **191**, 1–6.

127 T. Vossmeyer, E. DeIonno and J. R. Heath, *Angew. Chem., Int. Ed. Engl.*, 1997, **36**, 1080–1083.

128 D. J. Park, C. Zhang, J. C. Ku, Y. Zhou, G. C. Schatz and C. A. Mirkin, *Proc. Natl. Acad. Sci. U. S. A.*, 2015, **112**, 977–981.

129 Y. Zhang, J. Wang, Y. Zhao, J. Zhai, L. Jiang, Y. Song and D. Zhu, *J. Mater. Chem.*, 2008, **18**, 2650–2652.

130 H.-M. An, J. I. Sim, K. S. Shin, Y. M. Sung and T. G. Kim, *IEEE J. Quantum Electron.*, 2012, **48**, 891–896.

131 S. Furumi, H. Fudouzi, H. T. Miyazaki and Y. Sakka, *Adv. Mater.*, 2007, **19**, 2067–2072.

This journal is © The Royal Society of Chemistry 2021

J. Mater. Chem. C, 2021, **9**, 3368–3383 | **3383**